ACS OMEGA

http://pubs.acs.org/journal/acsodf

Article

Process Optimization for Catalytic Oxidation of Dibenzothiophene over UiO-66-NH_2 by Using a Response Surface Methodology

Bijan Barghi,* Martin Jürisoo, Maria Volokhova, Liis Seinberg, Indrek Reile, Valdek Mikli, and Allan Niidu

Cite This: *ACS Omega* 2022, 7, 16288−16297

Read Online

ACCESS | Metrics & More | Article Recommendations

ABSTRACT: This research investigates the catalytic performance of a metal−organic framework (MOF) with a functionalized ligand—UiO-66-NH_2—in the oxidative desulfurization of dibenzothiophene (DBT) in *n*-dodecane as a model fuel mixture (MFM). The solvothermally prepared catalyst was characterized by XRD, FTIR, ^{1}H NMR, SEM, TGA, and MP-AES analyses. A response surface methodology was employed for the experiment design and variable optimization using central composite design (CCD). The effects of reaction conditions on DBT removal efficiency, including temperature (X_1), oxidant agent over sulfur (O/S) mass ratio (X_2), and catalyst over sulfur (C/S) mass ratio (X_3), were assessed. Optimal process conditions for sulfur removal were obtained when the temperature, O/S mass ratio, and C/S mass ratio were 72.6 °C, 1.62 mg/mg, and 12.1 mg/mg, respectively. Under these conditions, 89.7% of DBT was removed from the reaction mixture with a composite desirability score of 0.938. From the results, the temperature has the most significant effect on the oxidative desulfurization reaction. The model *F* values gave evidence that the quadratic model was well-fitted. The reusability of the MOF catalyst in the ODS reaction was tested and demonstrated a gradual loss of activity over four runs.

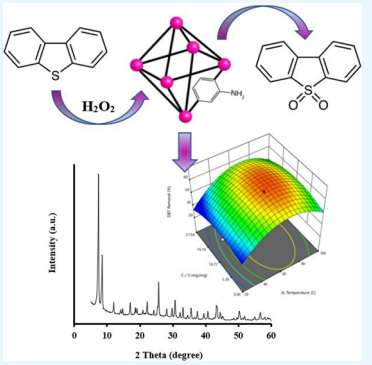

1. INTRODUCTION

Currently, the implementation by most countries of strict regulations for fossil fuels for environmental protection purposes has prompted a growing interest in investigations to improve deep desulfurization methodologies.[1−3] Hydrodesulfurization (HDS) is one of the most efficient methods in removing sulfur compounds;[4,5] nonetheless, it is less effective for removing planar sulfur-containing compounds, e.g., benzothiophene and dibenzothiophene. It requires large reactors and highly active catalysts with severe operating conditions, including high temperature and hydrogen pressure.[6,7] Hence, alternative approaches are required to achieve deep desulfurization, including selective adsorption, alkylative desulfurization, biodesulfurization, and oxidative desulfurization (ODS).[8] ODS is a green and promising process for removing planar sulfur compounds that can be carried out under ambient conditions while avoiding the use of hydrogen.[9] In an ODS reaction, when sulfur-containing compounds are oxidized, the sulfur removal efficiency of the catalysts is enhanced.[10,11] ODS converts sulfur compounds into high-polarity sulfoxides and sulfones that can be extracted by a polar solvent afterward. ODS reactions can be operated under mild operating conditions in the liquid phase.

Various oxidizing agents such as *tert*-butyl hydroperoxide, hydrogen peroxide, and oxygen have been addressed in prior studies.[12−14] However, hydrogen peroxide is the more favorable agent because of its commercial availability, selectivity, and environmental issues.[15−18] Employing an appropriate catalyst improves the activity of oxidants in the ODS process, of which metal−organic frameworks (MOFs) are good candidates that contain structurally rigid inorganic secondary building units (SBUs) and flexible and tunable organic linkers.[19−22] Among the hybrid MOFs, UiO-66(Zr) derivatives are impressively contributing to both scientific and industrial applications. It has been outlined that pristine UiO-66 can achieve more than 90% oxidative sulfur conversion in a short reaction time;[23−25] moreover, other functional groups (−NH_2, −OH) could also significantly influence the chemical activity and it has been mentioned that they can provide a strong affinity for sulfur oxidation.[26−29]

Presently, various MOFs have been recognized for ODS reactions, while there have been only a few reports on using amino-functionalized UiO-66. The performance of UiO-66-NH_2 was investigated for thiophene removal from *n*-octane at 40 °C with a certain amount of an MOF,[30] dibenzothiophene

Received: October 25, 2021
Accepted: March 29, 2022
Published: May 2, 2022

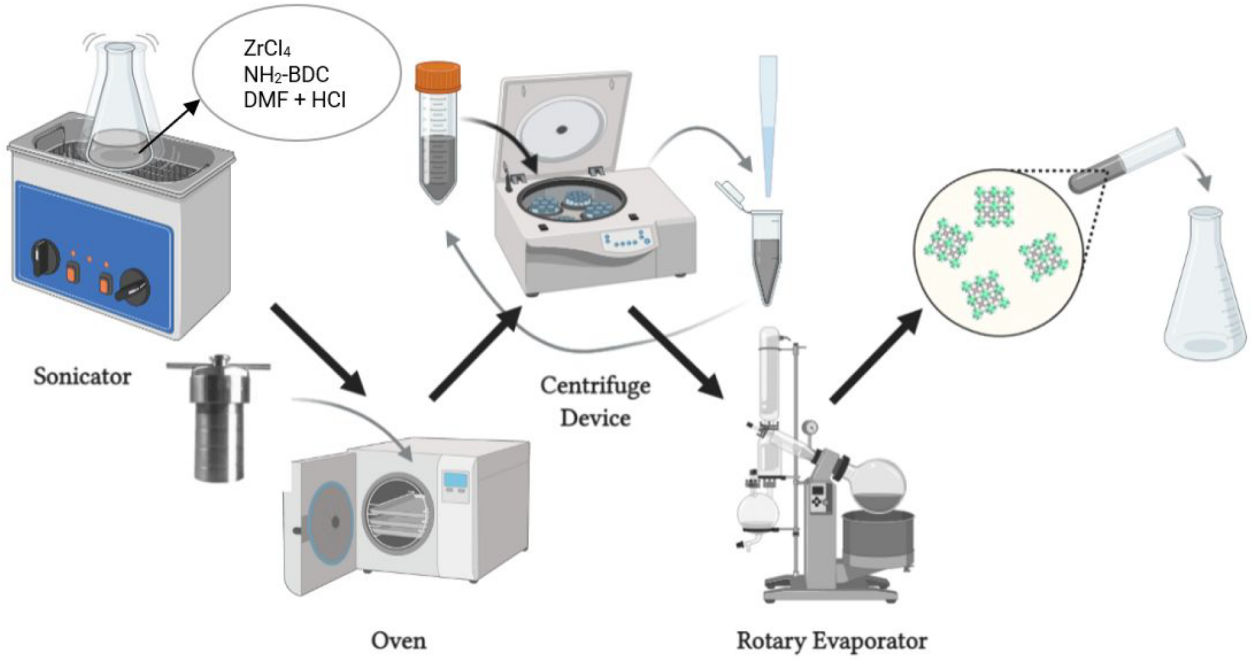

Figure 1. Schematic of the solvothermal synthesis of UiO-66-NH_2 (created with BioRender.com).

removal from *n*-octane at 70%°C with an H_2O_2/sulfur ratio of 4,[31] and DBT and 4,6-dimethyldibenzothiophene removal at 60 °C with an H_2O_2/sulfur ratio of 6 and 0.184 mmol of catalyst.[32] Thus, far, there have been no reports on statistical optimization of operation conditions and MOF amounts.

In this study, amino-functionalized (−NH_2) UiO-66(Zr) was synthesized by a solvothermal method for the ODS reaction. The characterization of samples was carried out by different techniques, including XRD, FTIR, ^{1}H NMR, SEM, TGA, and MP-AES. The effect of the reaction conditions and the performance of UiO-66-NH_2 in DBT oxidative removal were systematically investigated, leading to the development of optimal operational conditions. To understand the importance of process parameters—temperature, oxidant amount, and catalyst dosage—a quadratic statistical model was developed from which optimal conditions were derived by employing a response surface methodology (RSM).

2. EXPERIMENTAL SECTION

2.1. Materials. Zirconium(IV) chloride (ZrCl4, 98%, Acros), 2-aminoterephthalic acid (99%, Acros), hydrochloric acid (HCl, 36%, Honeywell), *N,N*-dimethylformamide (DMF, 99.5%, Fisher), ethanol (C_2H_5OH, 99.9%, Honeywell), acetonitrile (99.9%, Honeywell), *n*-dodecane (99%, Alfa Aesar), hydrogen peroxide (H_2O_2, 30%, Alfa Aesar), and dibenzothiophene (98%, Acros) were used as received.

2.2. Synthesis of UiO-66-NH_2. The UiO-66-NH_2 MOF was prepared as previously reported.[33] Briefly, 1 g of $ZrCl_4$ and 1.07 g of 2-aminoterephthalic acid (NH_2-BDC) were dissolved in a mixture of 120 mL of *N,N*-dimethylformamide (DMF) and 8 mL of concentrated HCl with sonication for 30 min. The obtained solution was placed in an oven at 80 °C for 24 h. After it was cooled to room temperature, the product was washed three times with DMF and three times with ethanol to remove all residual solvent. Then the sample was dried by heating to 80 °C under vacuum until a pressure of 600 mbar was reached. The synthesis procedure is depicted in Figure 1.

2.3. Characterization Methods. X-ray powder diffraction (XRD) patterns were measured on a Rigaku Ultima IV or Panalytic Powder3 diffractometer with a 1D strip detector and Cu Kα radiation (λ = 0,154 nm), a beam voltage of 45 kV, and a beam current of 40 mA. Patterns were collected in the range $5° < 2\theta < 50°$ with a 0.05° step size at a scanning rate of 1°/min. The functional moieties of the samples were characterized by Fourier transform infrared spectroscopy (Thermo Scientific Nicolet iS50 FTIR Spectrometric Analyzer) in the wavelength range of 400−4000 cm^{-1}. Scanning electron microscopy (SEM) images and surface elemental compositions of selected materials using EDS were obtained on a Zeiss FEG-SEM Ultra-55 instrument. The thermal stability of materials was tested by a simultaneous thermal analyzer (Mettler-Toledo TGA 1) in the temperature range 25−800 °C and at a heating rate of 10 °C min^{-1}. Microwave plasma atomic emission spectroscopy (MP-AES) with an Agilent 4200 microwave plasma atomic emission spectrometer was used to determine the purity of a sample and elemental ratios. Proton NMR spectroscopy of digested MOF samples was carried out on a 500 MHz Agilent DD2 instrument. The NMR spectrometer was equipped with a 5 mm 1D PFG probe head at 25 °C sample temperature. NMR analysis was used to determine the bulk purity of a MOF by digesting 1−2 mg of a sample in 5−10 drops of NaOD, sonicating the mixture until the sample was well dispersed, and then adding an appropriate amount of D_2O (650 uL).

2.4. Oxidative Desulfurization Process. Catalytic oxidative desulfurization of dibenzothiophene was carried out in a 6 dram reactor. For the polar phase 6 mL of acetonitrile and for the fuel phase (MFM) 6 mL of a solution of *n*-dodecane with 1000 ppm of dibenzothiophene were placed in a reactor, and by following the design of the experiment, the desired amount of the MOF as a catalyst was placed in the reactor. The glass batch reactor was equipped with a thermometer, magnetic stirrer, and an oil bath for temperature control. Upon heating of the reactor (20−100 °C), a specified amount of hydrogen peroxide was added at atmospheric pressure. The ODS reaction started after stirring the solution

https://doi.org/10.1021/acsomega.1c05965
ACS Omega 2022, 7, 16288−16297

(600 rpm) to decrease the limitation of mass transfer. According to the experiment design, the effects of three main variables, including reaction temperature, the mass ratio of oxidant to the total amount of sulfur, and MOF dosage, were examined. After completion of the reaction (150 min), samples from the fuel phase were taken and finally analyzed by a Shimadzu QP2010 plus gas chromatograph−mass spectrometer to obtain the DBT conversion. In this study, sulfones and sulfoxides were not analyzed. Equation 1 presents the calculation of efficiency of dibenzothiophene removal as the response of the design of experiments

$$\text{sulfur removal}\ (\%) = (C_0 - C_t)/C_0 \quad (1)$$

where C_0 and C_t refer to initial and final DBT (sulfur) concentrations in MFM, respectively.

2.5. Response Surface Methodology. To examine the effect of the designated variables on the output response, a central composite design (CCD) with a quadratic model was employed.[34] In this method, independent variables are coded at five levels: the central point is represented by 0, −1 and +1 are factorial points, and finally, $+\alpha$ and $-\alpha$ levels refer to axial points. An analysis of variance (ANOVA) was applied to statistically analyze the measured factors and their responses.[35] The coefficient of determination (R^2) was used to measure the variation between experimental and predicted responses in the quadratic model. The statistical significance of the proposed model was investigated by p and F values. The actual values of coded levels and the range of factors are given in Table 1. The

Table 1. Independent Test Variables at Five Levels Used for Central Composite Design

			coded variable level				
factor	unit	code	$(-\alpha^a)$	(−1)	(0)	(+1)	$(+\alpha^a)$
temp	°C	X_1	20	36.21	60	83.78	100
O/S ratio		X_2	0.5	1.61	3.25	4.89	6
C/S ratio		X_3	0.5	3.44	7.75	12.06	15

$^a\alpha$ = 1.68.

mathematical equation of the quadratic model is expressed in eq 2

$$Y = \beta_0 + \sum_{i=1}^{3} \beta_i X_i + \sum_{i=1}^{3}\sum_{j=1}^{3} \beta_{ij} X_i X_j + \varepsilon \quad (2)$$

where X_i and X_j are the coded values of variables, Y is output response, β_0, β_i, and β_{ij} indicate polynomial coefficients for the constant, linear and, interaction terms, respectively, and ε is the random error of the model. The actual number of experiments (N) is determined be eq 3

$$N = 2^k + 2k + n_0 \quad (3)$$

where k is the number of independent factors, 2^k is the number of experiments for the factorial points, $2k$ is the number of experiments for the axial points, and n_0 is the number of repetitions for the central points. On the basis of the CCD method, 17 test runs were performed for ODS reaction optimization. The CCD model was conducted using Design-Expert version 12 software.

3. RESULTS AND DISCUSSION

3.1. Characterization. As illustrated in Figure 2a, XRD was used to evaluate the structure, crystallinity, and phase purity of UiO-66-NH_2. The diffraction of this sample depicted the XRD patterns of the as-synthesized UiO-66-NH_2, which were identical to those of the reported XRD patterns and confirmed that UiO-66-NH_2 had been successfully prepared.[36,37] As shown in Figure 2a, the zirconium−benzene carboxylate units form an orthorombic crystal lattice with *Immm* space group, and the major diffraction peaks were characterized using a database (ICDD-JCPDS: 964132916). Also, it was confirmed that the sample does not have any byproducts.

FT-IR bands of the sample are presented in Figure 2b. For UiO-66-NH_2, the IR band at 1658 cm^{-1} was assigned to the C═O vibrations, indicating that DMF resides in the pores. The characteristic bands of O−C−O asymmetric stretching (at 1571 cm^{-1}) and symmetric stretching of terephthalic acid (1387 cm^{-1}) were also observed. In addition, spectral bands at 1491, 766, and 662 cm^{-1} were attributed to the vibration of C═C bonds of aromatic rings, and −OH and C−H vibrations in H_2BDC, respectively. Meanwhile, the peak at 1438 cm^{-1} could be ascribed to the N−H bending and C−N stretching vibrations.[38,39] Moreover, the IR spectrum of the sample

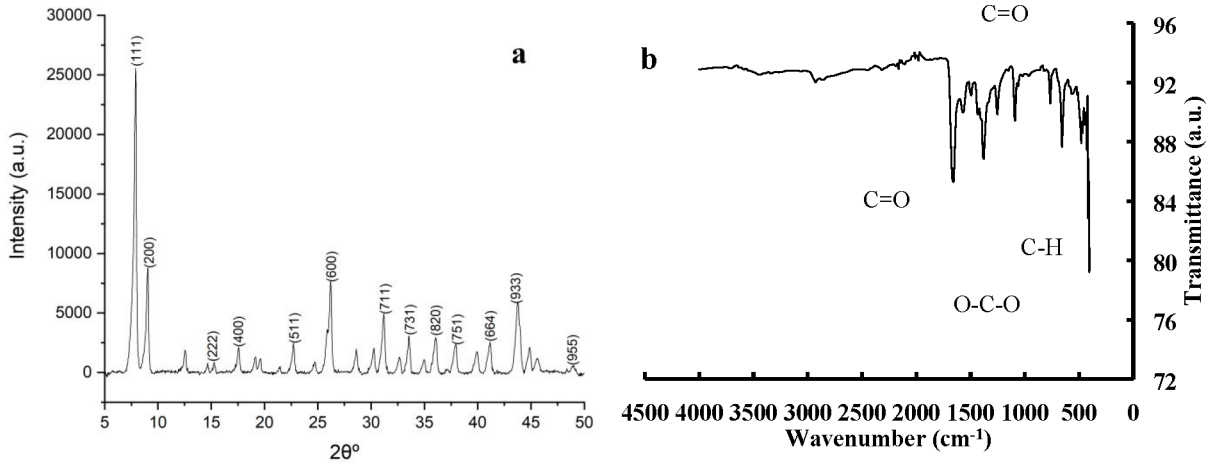

Figure 2. XRD powder pattern (a) and FT-IR spectrum (b) of UiO-66-NH_2.

https://doi.org/10.1021/acsomega.1c05965
ACS Omega 2022, 7, 16288−16297

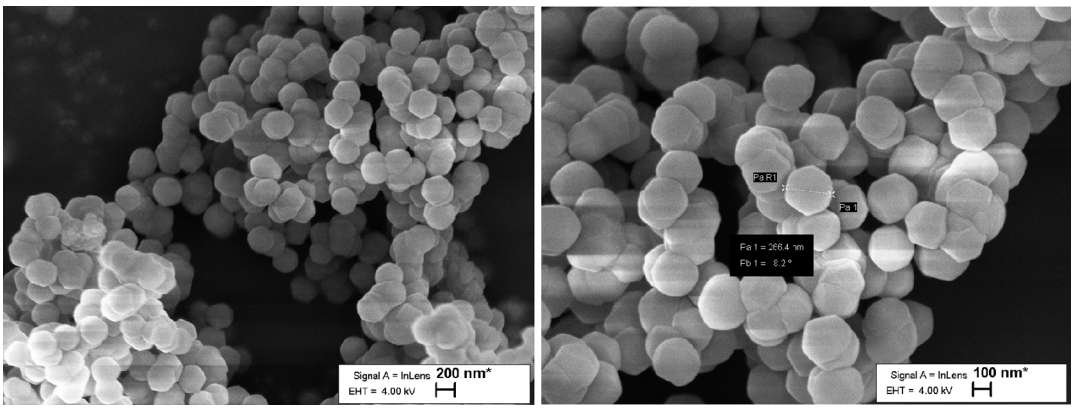

Figure 3. Typical SEM images of UiO-66-NH_2.

demonstrated one small absorption peak at 3631 cm^{-1}; this peak was ascribed to the $-NH_2$ group.[40]

From the SEM picture (Figure 3), the UiO-66-NH_2 samples were shown to exhibit a uniform octagonal morphology. On the basis of the images, the particle sizes generally converged at around 260 nm.

Figure 4 presents an ^1H NMR analysis for the synthesized UiO-66-NH_2 after digestion in an NaOD/D_2O solution. The

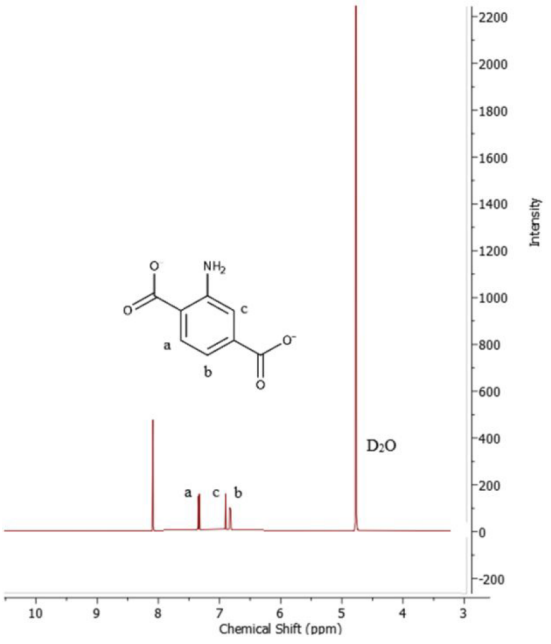

Figure 4. ^1H NMR spectrum of the prepared UiO-66-NH_2.

spectrum of UiO-66-NH_2 presents signals at 6.84, 6.90, and 7.35 ppm that were assigned to the benzene ring structure of the amino terephthalic acid in the MOF.[41]

A thermogravimetric analysis (TGA) curve of UiO-66-NH_2 is shown in Figure 5. The TGA curve demonstrated a three-step weight loss. The initial mass loss at 45−130 °C was assigned to the removal of ethanol and water; the second mass loss was from removal of DMF coordinated to Zr−O. The third step in weight loss after 500 °C was due to dehydroxylation of the zirconium oxo clusters and framework decomposition.[42] A quantitative analysis (MP-AES) of UiO-66-NH_2 showed that the zirconium composition was 25.1% of the MOF.

3.2. Statistical Analysis. Experiments were carried out according to the specified experimental design based on a central composite design procedure. The designated parameters, including the reaction temperature, the oxidant to sulfur mass ratio (O/S), and the catalyst to sulfur mass ratio (C/S), were studied at the designated reaction time. Accordingly, independent factors, predicted values, and experimental responses are given in Table 2. The equation in terms of actual factors as a quadratic model is obtained as shown in eq 4:

$$\begin{aligned}\text{DBT removal (wt \%)} &= -25.99 + 2.56X_1 + 11.13X_2 + 2.30X_3 - 0.09X_1X_2 \\ &\quad + 0.006X_1X_3 - 0.25X_2X_3 - 0.017{X_1}^2 - 0.52{X_2}^2 \\ &\quad - 0.10{X_3}^2 \end{aligned} \quad (4)$$

The fitness of the quadratic model was evaluated by the coefficient of determination (R^2), and its multiple regression model was investigated by an F test. An analysis of variance (ANOVA) was performed for the fitted quadratic polynomial model of DBT removal. As demonstrated in Table 3, the model F value of 7.79 implies that there is only a 0.65% chance that such a large F value could occur due to noise. Also, the model P value of less than 0.05 showed that the model is statistically significant. The F value for the lack of fit (6.46) means that it is not significant relative to the pure error. There is a 13.96% chance that a lack of fit F value this large could occur due to noise; thus, it is not significant. A nonsignificant lack of fit means the model is correctly fitted to the data and corroborated by the coefficient of determination value (R^2 = 0.914), indicating that the predicted mathematical model was well-fitted to the experimental data.

A comparison of the observed and predicted responses is illustrated in Figure 6; the plot depicts the reliability of the model, which implies that the DBT removal correlation has high accuracy within the investigated range of variables (eq 4).

Figure 7 proves the reliability of the predicted model by normal percent probability plot of the residuals. The straight line of the graph obviously demonstrates that the residuals show a normal distribution.

This research was conducted to determine the effect of individual parameters and their interactions by using the benefit of the design of experiment (DOE). The significance of each of the three independent parameters (temperature, O/S mass ratio, and C/S mass ratio) on DBT removal efficiency

https://doi.org/10.1021/acsomega.1c05965
ACS Omega 2022, 7, 16288−16297

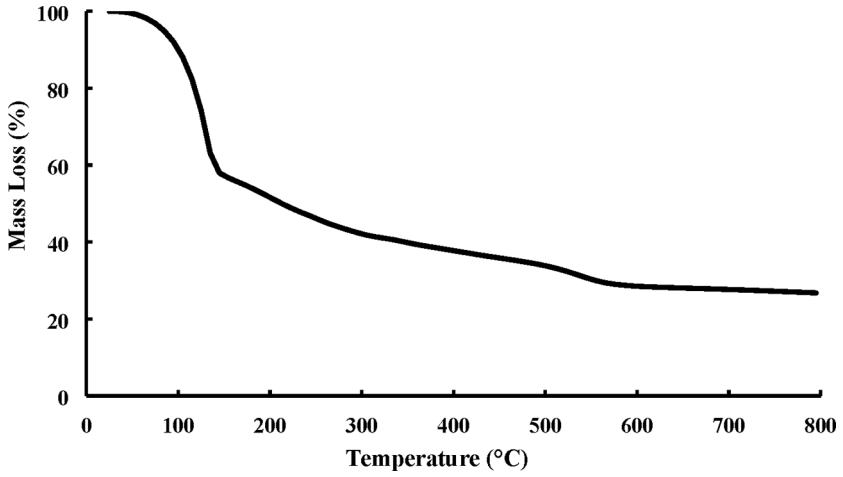

Figure 5. TGA curve of pristine UiO-66-NH_2 (N_2 atmosphere, heating rate 10 °C/min).

Table 2. Central Composite Design Arrangement and Predicted and Experimental Responses

					DBT removal efficiency (%)	
run no.	point type	X_1 (°C)	X_2 (mg/mg)	X_3 (mg/mg)	predicted	experimental
1	center	60.00	3.25	7.75	87.41	89.02
2	axial	36.22	4.89	3.44	73.44	73.14
3	axial	83.78	4.89	12.06	77.97	77.81
4	factorial	60.00	0.50	7.75	82.62	78.86
5	axial	83.78	1.61	12.06	87.58	92.63
6	factorial	100.00	3.25	7.75	70.29	67.60
7	axial	83.78	1.61	3.44	79.83	79.31
8	factorial	60.00	3.25	0.50	79.80	77.27
9	center	60.00	3.25	7.75	87.41	85.18
10	axial	36.22	4.89	12.06	71.74	77.03
11	factorial	60.00	6.00	7.75	84.40	81.43
12	axial	36.22	1.61	3.44	61.71	66.62
13	axial	83.78	4.89	3.44	77.24	81.26
14	center	60.00	3.25	7.75	87.41	89.18
15	factorial	20.00	3.25	7.75	49.81	45.77
16	factorial	60.00	3.25	15.00	84.89	80.70
17	axial	36.22	1.61	12.06	67.03	67.77

Table 3. ANOVA for Polynomial Model of Dibenzothiophene Oxidation Yield[a]

source	sum of squares	degree of freedom	mean square	*F* value	*P* value
A: temp (°C)	506.24	1	506.24	20.16	0.0028
B: O/S (mg/mg)	3.84	1	3.84	0.1527	0.7076
C: C/S (mg/mg)	31.27	1	31.27	1.25	0.3013
AB	102.53	1	102.53	4.08	0.0831
AC	2.92	1	2.92	0.1162	0.7432
BC	24.64	1	24.64	0.9809	0.3550
A^2	1054.84	1	1054.84	42.00	0.0003
B^2	21.46	1	21.46	0.8543	0.3861
C^2	36.09	1	36.09	1.44	0.2696
model	1760.22	9	195.58	7.79	0.0065
lack of fit	165.56	5	33.11	6.46	0.1396
error	10.26	2	5.13		

[a] R^2 = 91.37%; adjusted R^2 = 89.27%.

was specified by indicating the 3D surface plots and response contours (Figures 8 and 9). Figure 8 depicts response surface plots between the oxidation temperature reaction and the oxidant to sulfur mass ratio on the ODS of dibenzothiophene, which demonstrates that both factors have noticeable effects on the removal efficiency of DBT. It was observed that at a certain temperature, as the oxidant/sulfur mass ratio increases to 1.7, first the dibenzothiophene ODS efficiency is enhanced and afterward is decreased by oxidant/sulfur ratio ≥8 and higher. However, the dibenzothiophene oxidation yield

https://doi.org/10.1021/acsomega.1c05965
ACS Omega 2022, 7, 16288−16297

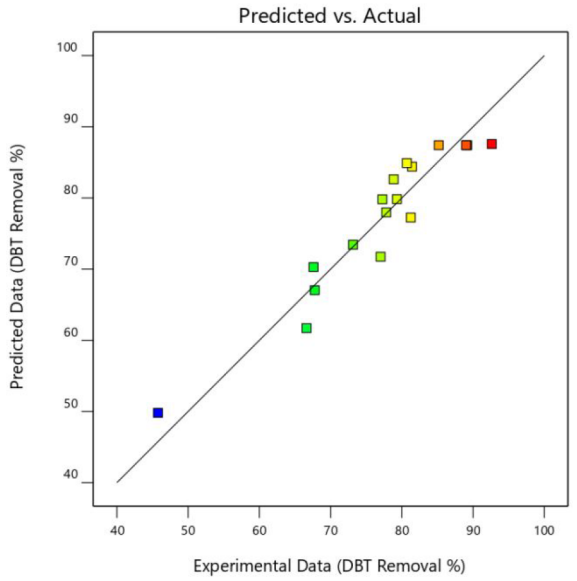

Figure 6. experimental and predicted removal yield of dibenzothiophene.

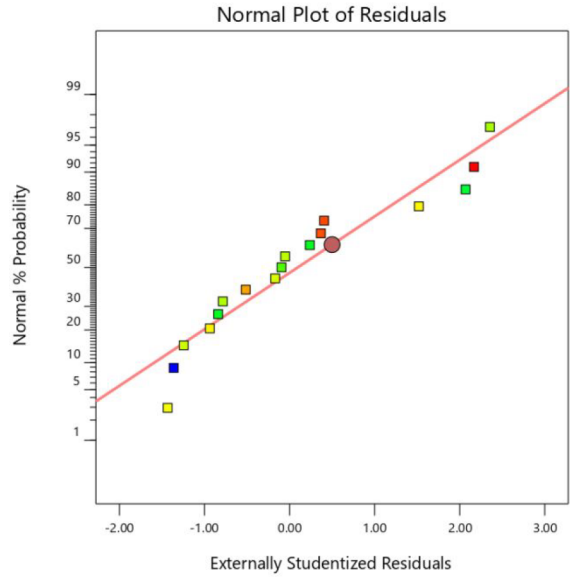

Figure 7. Normal percent probability versus Studentized residuals plot for the model.

increased in the presence of greater amounts of oxidants;[43,44] greater amounts of oxidants generate water molecules due to decomposition, which may occupy the MOF surface area and diminish the adsorption of dibenzothiophene on active sites. In addition, economic and environmental issues to decrease the utilization of oxidants should always be considered. Thus, the model calculated the optimal amount O/S = 1.62 mg/mg for the ODS reaction.

Increasing the temperature of the reaction from 60 to 72 °C induces an enhanced dibenzothiophene oxidation yield for a certain oxidant/sulfur mass ratio; however, temperature increases above 72 °C reduced the dibenzothiophene oxidation efficiency. As the oxidative desulfurization reaction is endothermic,[45] temperature enhancement is favors the dibenzothiophene removal process rate as well as increases the molecular movement of reaction components. On the other hand, increasing the temperature leads to oxygen peroxide decomposition; consequently, as the oxidant concentration is decreased, the ODS reaction rate is reduced.[46] Therefore, the optimal temperature can be considered to be 72 °C.

Figure 9 demonstrates the binary interaction of reaction temperature and C/S ratio. Obviously, at C/S ratios of 0.5−12 and temperatures of 60−72 °C, the maximum efficiency of dibenzothiophene ODS was attained that is pertinent to nearly complete removal, indicating that a catalyst/sulfur (C/S) ratio of 12 increased the concentration of MOF active sites at a proper level, which led to a greater dibenzothiophene oxidation yield. However, excess amounts of the MOF lead to agglomeration and active site reduction, limit the surface area with the absorbate, and negatively affect the mass transfer of reactants, and finally the efficiency of MOF catalytic activity for the oxidation process is decreased.[47]

3.3. Determination of Optimal Conditions. The central composite design technique has been employed to determine the optimal conditions of UiO-66-NH_2 MOF preparation for the oxidative dibenzothiophene removal to be maximized from MFM. Table 4 displays the optimal conditions for maximum DBT removal with a desirability value of 0.938 for the determined values of the three independent factors.

Table 5 shows the effect of UiO-66-NH_2 on oxidative desulfurization performance with and without catalyst. It was studied by keeping the O/S ratio 1.6, stirrer speed constant at 600 rpm, 6 mL of model fuel, 6 mL of acetonitrile, 1000 ppm of DBT, for 150 min at 36.2, 60.0, 72.6, and 83.8 °C temperatures. In the case of without catalyst (just extraction effect), the sulfur removal was about 43%, 55%, 56% and 56% less than reaction condition in the presence of the catalyst.

3.4. Proposed Mechanism. Figure 10 shows a plausible mechanism for the dibenzothiophene catalytic oxidative reaction. Metal cluster units of the UiO-66-NH_2 structure $[Zr_6O_4(OH)_4]$ are connected to 12 rings of amino terephthalic acid; accordingly, the MOF is able to strengthen the electrophilicity property of the oxidant with high electron-withdrawing capability and a reduced number of $Zr^{\delta+}$ sites. These active sites are able to increase the electrophilicity of the H_2O_2 in sulfur removal.[17] In the first step of the mechanism, the Zr−OH sites were protonated and then dehydrated to form unsaturated Zr sites. The unsaturated Zr sites serving as Lewis acids react with oxygen peroxide to generate peroxometallic Zr complexes in an oxidation reaction.[15] Zr ions on the MOF surface coordinated with the sulfur adsorb on the Lewis acid sites,[24] where their existence has been proven in UiO-66 and its derivatives in previous studies.[15,48,49] It has also been reported that UiO-66-NH_2 has many more Lewis acid sites in comparison to UiO-66.[49] The reaction between a Zr−O ion and an oxygen of the peroxide leads to hydroxyl radicals formation; accordingly, $^{\bullet}OH$ radicals have high oxidizability and electrophilicity as active oxygen species. During the electrophilic oxidation, two protons of the dibenzothiophene sulfur atom shift when the atom nucleophilically attacks the oxidative agent, and then a sulfoxide intermediate forms when the oxygen atom is transferred to the planar sulfur molecule. The generated sulfoxide forms a hydrogen bond with the active sites of ZrOH, decreasing the electronic density of the sulfur atom in the sulfoxide and thus activating it for the next nucleophilic attack by the oxidizing agent, finally leading to sulfone formation.[15,50] The ODS reaction can also occur without catalyst, but with less removal

https://doi.org/10.1021/acsomega.1c05965
ACS Omega 2022, 7, 16288−16297

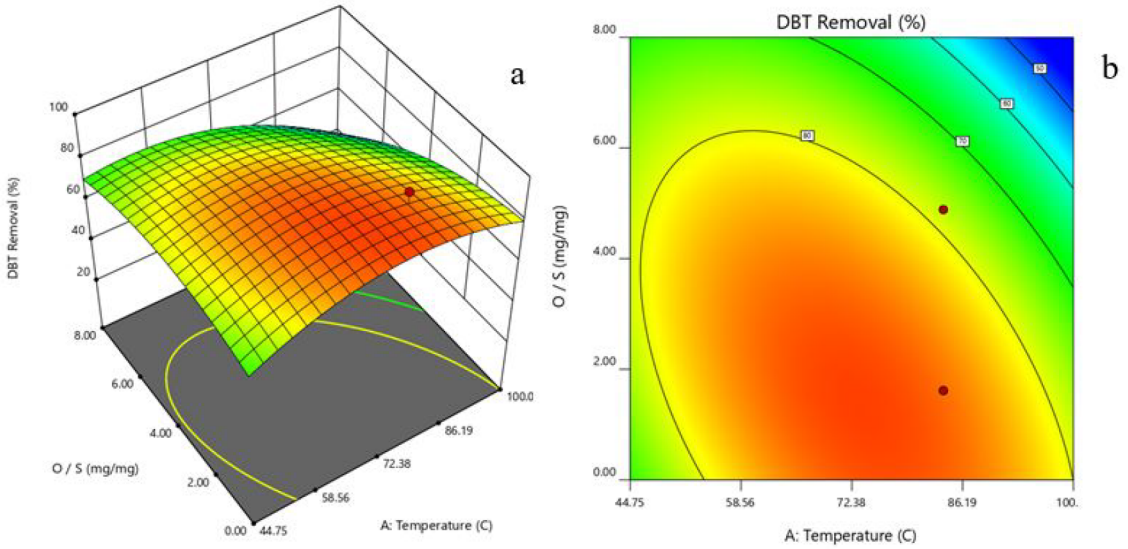

Figure 8. Response surface three-dimensional (a) and two-dimensional contour plots (b) indicating the effect of the reaction temperature versus oxidant/sulfur mass ratio on the dibenzothiophene oxidation efficiency. X_3 = 12 mg of MOF/mg of sulfur.

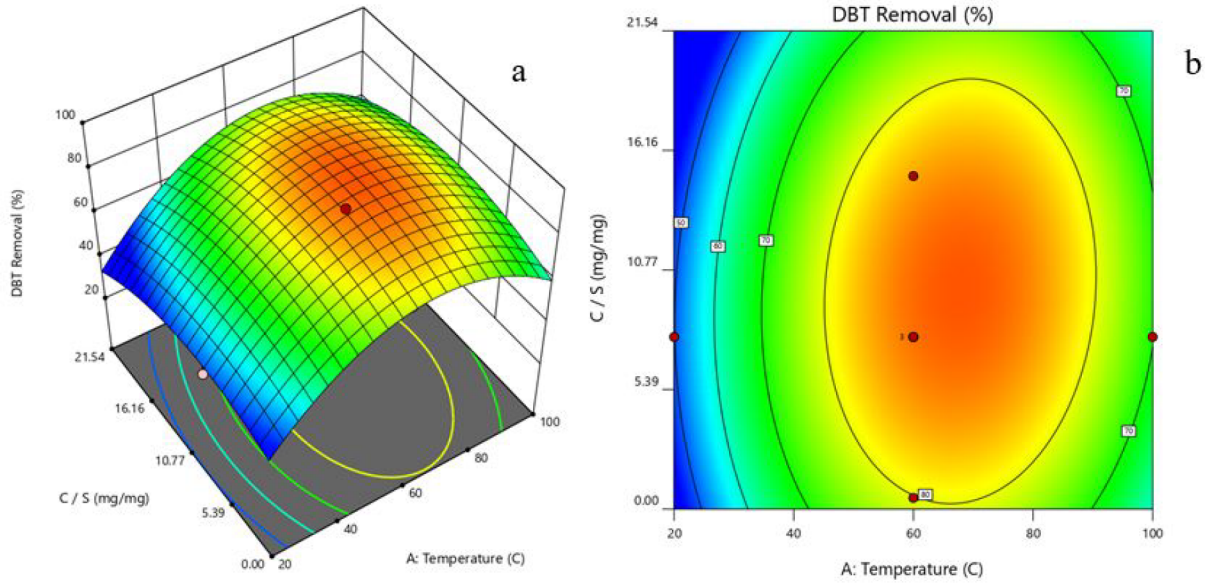

Figure 9. Response surface three-dimensional (a) and two-dimensional contour plots (b) indicating the effect of the reaction temperature versus catalyst/sulfur mass ratio on the dibenzothiophene oxidation efficiency. X_2 = 1.6 mg of oxidant/mg of sulfur.

Table 4. Predicted Value Obtained for DBT Removal under Optimum Conditions

independent factor		dibenzothiophene removal efficiency (%)	desirability (%)
A: temp (°C)	72.6	89.7	93.8
B: O/S ratio	1.62		
C: C/S ratio	11.03		

Table 5. DBT Removal with and without UiO-66-NH_2 in the Presence of H_2O_2

	DBT removal at different temperatures (%)			
	36.2 °C	60.0 °C	72.6 °C	83.8 °C
UiO-66-NH_2 (13.5 mg)	68.2	87.0	89.7	89.6
no catalyst	25.1	32.1	33.7	33.6

efficiency. The benefit of the UiO-66-NH_2 MOF as a catalyst not only is due to the high activation of peroxide hydrogen inner bonds through the formation of $O^{\bullet-}{}_2$ and $^{\bullet}OH$ radicals but also the MOF mechanical stability for reuse in the ODS reaction results in a higher sulfur removal efficiency.[51]

When oxygen peroxide is employed as an oxidation agent, the catalytic activity of UiO-66-NH_2 depends on its ability to decompose H_2O_2 into $O^{\bullet-}{}_2$ and $^{\bullet}OH$ radicals (oxygen species).[52] The UiO-66 structure includes open metal nodes occupied by hydroxide or water as a terminal ligand to form Zr−OH and Zr−OH_2. Introduction of an amino group (−NH_2) as an electron-donating group in the terephthalic acid linker can enhance the decomposition of hydrogen peroxide, thus initiating the proton donation to Zr sites.[26] Furthermore, the adsorption of sulfur compounds is affiliated

https://doi.org/10.1021/acsomega.1c05965
ACS Omega 2022, 7, 16288−16297

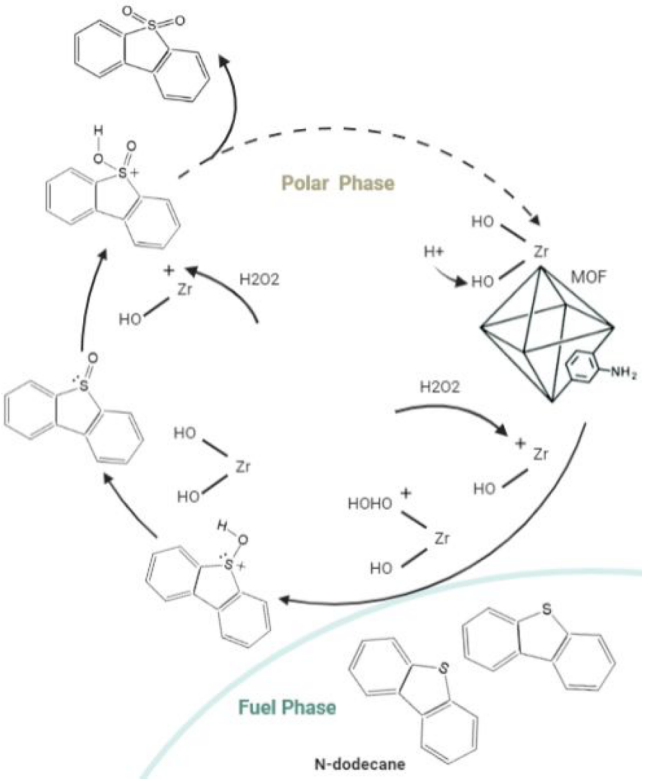

Figure 10. Plausible mechanism for the dibenzothiophene ODS reaction in the presence of the UiO-66-NH_2 MOF and H_2O_2 (created with BioRender.com).

with the H atom bonding. Dibenzothiophene with electron pairs around the sulfur atom is a H acceptor; consequently, an amino group in UiO-66 as a H-donor species improves the adsorption performance.[26,53]

3.5. Reusability of Spent Metal Organic Framework.

Catalyst reusability is a desirable property with regard to industrial utilization and economic evaluation. The regeneration of UiO-66-NH_2 catalysts was examined by performing four multiple DBT removal experiments at 72.6 °C under the optimal conditions. After each experiment, the MOF was separated from the oil phase and recovered by centrifugation. To eliminate the remaining sulfur, the used MOF was washed three times with acetonitrile and then dried at 100 °C in an oven for 12 h; the MOF was then utilized in a subsequent DBT removal reaction. Figure 11 illustrates the dibenzothiophene ODS yield, which was maintained at the initial level with a slight decreasing trend (about 8.5%) after four sequential cycles, decreasing from 90.08% to 82.45%. The gradual decrease in the MOF performance for the fourth cycle might be due to the fouling of MOF pores and decreasing number of active sites. Within the oxidative catalytic reaction, the formation of sulfone and sulfoxide may lead to MOF catalytic deactivation during π-complexation, so that washing and heating through the recovery process is not convenient to simply remove the poisonous agents.[54]

4. CONCLUSION

Functionalized UiO-66(Zr) was successfully synthesized through ligand substitution by a solvothermal methodology. The structure and phase purity of the MOF catalyst were confirmed by multiple characterization techniques. The effect

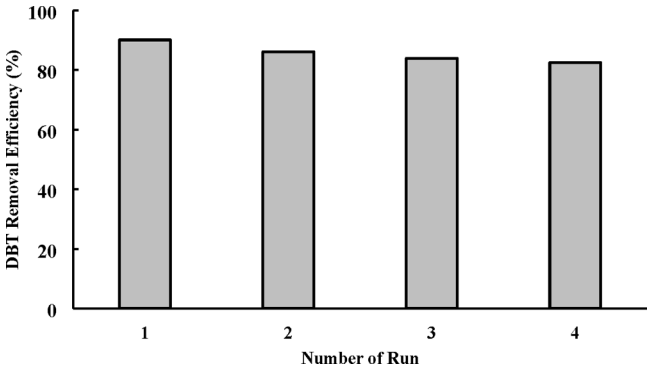

Figure 11. Reusability of the UiO-66-NH_2 catalyst in dibenzothiophene removal efficiency. Conditions: 6 mL of model fuel, 13.5 mg of MOF (C/S = 11.03), O/S = 1.6, 6 mL of acetonitrile, 150 min, 72.6 °C.

of the reaction conditions on dibenzothiophene ODS was examined, including the reaction temperature, oxidation agent/sulfur mass ratio, and catalyst/sulfur mass ratio, using the RSM-CCD technique. According to the values of the design point of desulfurization yields, the experimental results were fitted at an acceptable level to the predicted data with an appropriate R^2 value (about 5% error). The sulfur removal efficiency could reach 89.7% for 72.6 °C, an O/S ratio of 1.62, and a C/S ratio of 11.03 for DBT MFM (1000 ppm of S content), which was guaranteed by a desirability value of 0.938. According to the results, the temperature has the greatest effect on DBT removal; however, it seems that thermal decomposition of oxygen peroxide led to increasing oxidant usage and decreasing DBT removal at temperatures higher than 72.6 °C. Additionally, the DBT removal efficiency of the regenerated catalyst demonstrated that the employed MOF has acceptable reusability and retains its activity after four runs with about an 8.5% drop in the conversion of DBT.

AUTHOR INFORMATION

Corresponding Author

Bijan Barghi − *Virumaa College, School of Engineering, Tallinn University of Technology, 30322 Kohtla-Järve, Estonia;* orcid.org/0000-0001-9577-3302; Email: bijan.barghi@taltech.ee

Authors

Martin Jürisoo − *Virumaa College, School of Engineering, Tallinn University of Technology, 30322 Kohtla-Järve, Estonia*

Maria Volokhova − *National Institute of Chemical Physics and Biophysics, 12618 Tallinn, Estonia*

Liis Seinberg − *National Institute of Chemical Physics and Biophysics, 12618 Tallinn, Estonia*

Indrek Reile − *National Institute of Chemical Physics and Biophysics, 12618 Tallinn, Estonia;* orcid.org/0000-0003-3278-7947

Valdek Mikli − *Department of Chemistry and Materials Technology, School of Engineering, Tallinn University of Technology, 19086 Tallinn, Estonia*

Allan Niidu − *Virumaa College, School of Engineering, Tallinn University of Technology, 30322 Kohtla-Järve, Estonia;* orcid.org/0000-0003-3406-9869

Complete contact information is available at: https://pubs.acs.org/10.1021/acsomega.1c05965

https://doi.org/10.1021/acsomega.1c05965
ACS Omega 2022, 7, 16288−16297

Notes

The authors declare no competing financial interest.

■ ACKNOWLEDGMENTS

The authors appreciate the support of the Faculty of Engineering, Virumaa College of Tallinn University of Technology, and are thankful to Stat-Ease, Minneapolis, MN, USA, for providing the Design-Expert 12 Package. The authors acknowledge financial support from the Estonian Research Council (grant nos. PSG11 and PRG4) and from SA Archimedes of the European Regional Development Fund (project no. TK134).

■ REFERENCES

(1) Huang, C.; Chen, B.; Zhang, J.; Liu, Z.; Li, Y. Desulfurization of gasoline by extraction with new ionic liquidss. *Energy Fuels* **2004**, *18*, 1862−1864.
(2) Toutov, A. A.; Salata, M.; Fedorov, A.; Yang, Y.-F.; Liang, Y.; Cariou, R.; Betz, K. N.; Couzijn, E. P. A.; Shabaker, J. W.; Houk, K. N.; Grubbs, R. H. A potassium tert-butoxide and hydrosilane system for ultra-deep desulfurization of fuels. *Nat. Eng.* **2017**, 1−7.
(3) Li, S. S.; Li, Y. X.; Jin, M. M.; Miao, K. J.; Gu, M. X.; Liu, X. Q.; Sun, L. B. Controllable fabrication of cuprous sites in confined spaces for efficient adsorptive desulfurization. *Fuel* **2020**, *259*, 116221.
(4) Muhammad, Y.; Rashid, H. U.; Subhan, S.; Rahman, A. U.; Sahibzada, M.; Tong, Z. Boosting the hydrodesulfurization of dibenzothiophene efficiency of Mn decorated (Co/Ni)-Mo/Al_2O_3 catalysts at mild temperature and pressure by coupling with phosphonium based ionic liquids. *Chem. Eng. J.* **2019**, *375*, 121957.
(5) Shafiq, I.; Shafique, S.; Akhter, P.; Yang, W.; Hussain, M. Recent developments in alumina supported hydrodesulfurization catalysts for the production of sulfur-free refinery products: A technical review. *Catal. Rev.* **2022**, *64*, 1−86.
(6) Liu, Y.; Wang, H.; Zhao, J.; Liu, Y.; Liu, C. Ultra-deep desulfurization by reactive adsorption desulfurization on copper-based catalysts. *Energy Chem. J.* **2019**, *29*, 8−16.
(7) Rajendran, A.; Cui, T. Y.; Fan, H. X.; Yang, Z. F.; Feng, J.; Li, W. Y. A comprehensive review on oxidative desulfurization catalysts targeting clean energy and environment. *J. Mater. Chem. A A* **2020**, *8*, 2246−2285.
(8) Kang, L.; Liu, H.; He, H.; Yang, C. Oxidative desulfurization of dibenzothiophene using molybdenum catalyst supported on Ti-pillared montmorillonite and separation of sulfones by filtration. *Fuel* **2018**, *234*, 1229−1237.
(9) Gu, Q.; Wen, G.; Ding, Y.; Wu, K. H.; Chen, C.; Su, D. Reduced graphene oxide: a metal-free catalyst for aerobic oxidative desulfurization. *Green Chem.* **2017**, *19*, 1175−1181.
(10) Yu, X.; Han, P.; Li, Y. Oxidative desulfurization of dibenzothiophene catalyzed by α-MnO_2 nanosheets on palygorskite using hydrogen peroxide as oxidant. *RSC Adv.* **2018**, *8*, 17938−17943.
(11) Jiang, Z.; Hongying, L. Ü.; Zhang, Y.; Can, L. I. Oxidative desulfurization of fuel oilss. *Chin. J. Catal.* **2011**, *32*, 707−715.
(12) Gao, Y.; Gao, R.; Zhang, G.; Zheng, Y.; Zhao, J. Oxidative desulfurization of model fuel in the presence of molecular oxygen over polyoxometalate based catalysts supported on carbon nanotubes. *Fuel* **2018**, *224*, 261−270.
(13) Mokhtar, W. N. A. W.; Bakar, W. A. W. A.; Ali, R.; Kadir, A. A. A. Optimization of oxidative desulfurization of Malaysian Euro II diesel fuel utilizing tert-butyl hydroperoxide-dimethylformamide system. *Fuel* **2015**, *161*, 26−33.
(14) Jiang, X.; Li, H.; Zhu, W.; He, L.; Shu, H.; Lu, J. Deep desulfurization of fuels catalyzed by surfactant-type decatungstates using H_2O_2 as oxidant. *Fuel* **2009**, *88*, 431−436.
(15) Zheng, H. Q.; Zeng, Y. N.; Chen, J.; Lin, R. G.; Zhuang, W. E.; Cao, R.; Lin, Z. J. Zr-based metal-organic frameworks with intrinsic peroxidase-like activity for ultradeep oxidative desulfurization: mechanism of H_2O_2 decomposition. *Inorg. Chem.* **2019**, *58*, 6983−6992.
(16) Yu, G.; Lu, S.; Chen, H.; Zhu, Z. Oxidative desulfurization of diesel fuels with hydrogen peroxide in the presence of activated carbon and formic acid. *Energy Fuels* **2005**, *19*, 447−452.
(17) Hao, L.; Hurlock, M. J.; Ding, G.; Zhang, Q. Metal-organic frameworks towards desulfurization of fuels. *Met. Org. Framework* **2020**, *378*, 175−202.
(18) Chandra Srivastava, V. An evaluation of desulfurization technologies for sulfur removal from liquid fuels. *RSC Adv.* **2012**, *2*, 759−783.
(19) Bhadra, B. N.; Jhung, S. H. Oxidative desulfurization and denitrogenation of fuels using metal-organic framework-based/-derived catalysts. *Appl. Catal. B: Environ.* **2019**, *259*, 118021.
(20) Howarth, A. J.; Peters, A. W.; Vermeulen, N. A.; Wang, T. C.; Hupp, J. T.; Farha, O. K. Best practices for the synthesis, activation, and characterization of metal-organic frameworks. *Chem. Mater.* **2017**, *29*, 26−39.
(21) Smolders, S.; Willhammar, T.; Krajnc, A.; Sentosun, K.; Wharmby, M. T.; Lomachenko, K. A.; Bals, S.; Mali, G.; Roeffaers, M. B.; De Vos, D. E.; Bueken, B. A Titanium (IV)-Based Metal-Organic Framework Featuring Defect-Rich Ti-O Sheets as an Oxidative Desulfurization Catalyst. *Angew. Chem.* **2019**, *131*, 9258−9263.
(22) Gascon, J.; Corma, A.; Kapteijn, F.; Llabres i Xamena, F. X. Metal organic framework catalysis: quo vadis? *Acs Catal.* **2014**, *4*, 361−378.
(23) Ye, G.; Qi, H.; Li, X.; Leng, K.; Sun, Y.; Xu, W. Enhancement of oxidative desulfurization performance over UiO-66 (Zr) by titanium ion exchange. *ChemPhysChem* **2017**, *18*, 1903−1908.
(24) Zhang, X.; Huang, P.; Liu, A.; Zhu, M. A metal-organic framework for oxidative desulfurization: UIO-66 (Zr) as a catalyst. *Fuel* **2017**, *209*, 417−423.
(25) Viana, A. M.; Ribeiro, S. O.; Castro, B. D.; Balula, S. S.; Cunha-Silva, L. Influence of UiO-66 (Zr) preparation strategies in its catalytic efficiency for desulfurization process. *Mater.* **2019**, *12*, 3009.
(26) Zhang, X. F.; Wang, Z.; Feng, Y.; Zhong, Y.; Liao, J.; Wang, Y.; Yao, J. Adsorptive desulfurization from the model fuels by functionalized UiO-66 (Zr). *Fuel* **2018**, *234*, 256−262.
(27) Peterson, G. W.; Mahle, J. J.; DeCoste, J. B.; Gordon, W. O.; Rossin, J. A. Extraordinary NO_2 Removal by the Metal-Organic Framework UiO-66-NH_2. *Angew. Chem.* **2016**, *128*, 6343−6346.
(28) Zhang, J.; Hu, Y.; Qin, J.; Yang, Z.; Fu, M. TiO_2-UiO-66-NH_2 nanocomposites as efficient photocatalysts for the oxidation of VOCs. *Chem. Eng. J.* **2020**, *385*, 123814.
(29) Ye, G.; Qi, H.; Zhou, W.; Xu, W.; Sun, Y. Green and scalable synthesis of nitro-and amino-functionalized UiO-66 (Zr) and the effect of functional groups on the oxidative desulfurization performance. *Inorg. Chem. Front.* **2019**, *6*, 1267−1274.
(30) Wu, F.; Cao, Y.; Liu, H.; Zhang, X. High-performance UiO-66-NH_2 tubular membranes by zirconia-induced synthesis for desulfurization of model gasoline via pervaporation. *J. Membr. Sci.* **2018**, *556*, 54−65.
(31) Liao, X.; Wang, X.; Wang, F.; Yao, Y.; Lu, S. Ligand Modified Metal Organic Framework UiO-66: A Highly Efficient and Stable Catalyst for Oxidative Desulfurization. *J. Inorg. Organom. Polym. Mater.* **2021**, *31*, 756−762.
(32) Li, Z.; Liao, F.; Jiang, F.; Liu, B.; Ban, S.; Chen, G.; Sun, C.; Xiao, P.; Sun, Y. Capture of H_2S and SO_2 from trace sulfur containing gas mixture by functionalized UiO-66 (Zr) materials: A molecular simulation study. *Fluid Phase Equilib.* **2016**, *427*, 259−267.
(33) Katz, M. J.; Brown, Z. J.; Colón, Y. J.; Siu, P. W.; Scheidt, K. A.; Snurr, R. Q.; Hupp, J. T.; Farha, O. K. A facile synthesis of UiO-66, UiO-67 and their derivatives. *Chem. Commun.* **2013**, *49*, 9449−9451.
(34) Barghi, B.; Niidu, A.; Karimzadeh, R. The effect of water and zinc loading on LPG catalytic cracking for light olefin production using Response Surface Methodology. *Proc. Est. Acad. Sci.* **2021**, *70*, 135−147.

https://doi.org/10.1021/acsomega.1c05965
ACS Omega 2022, 7, 16288−16297

(35) Bezerra, M. A.; Santelli, R. E.; Oliveira, E. P.; Villar, L. S.; Escaleira, L. A. Response surface methodology (RSM) as a tool for optimization in analytical chemistry. *Talanta* **2008**, *76*, 965−977.
(36) Zlotea, C.; Phanon, D.; Mazaj, M.; Heurtaux, D.; Guillerm, V.; Serre, C.; Horcajada, P.; Devic, T.; Magnier, E.; Cuevas, F.; Ferey, G.; Llewellyn, P. L.; Latroche, M. Effect of NH_2 and CF_3 functionalization on the hydrogen sorption properties of MOFs. *Dalton Trans.* **2011**, *40*, 4879−4881.
(37) Sadeghi, S.; Jafarzadeh, M.; Abbasi, A. R.; Daasbjerg, K. Incorporation of CuO NPs into modified UiO-66-NH_2 metal-organic frameworks (MOFs) with melamine for catalytic C-O coupling in the Ullmann condensation. *New J. Chem.* **2017**, *41*, 12014−12027.
(38) Vermoortele, F.; Ameloot, R.; Vimont, A.; Serre, C.; De Vos, D. An amino-modified Zr-terephthalate metal-organic framework as an acid-base catalyst for cross-aldol condensation. *Chem. Commun.* **2011**, *47*, 1521−1523.
(39) Vermoortele, F.; Vandichel, M.; Van de Voorde, B.; Ameloot, R.; Waroquier, M.; Van Speybroeck, V.; De Vos, D. E. Electronic effects of linker substitution on Lewis acid catalysis with metal-organic frameworks. *Angew. Chem., Int. Ed.* **2012**, *51*, 4887−4890.
(40) Shearer, G. C.; Forselv, S.; Chavan, S.; Bordiga, S.; Mathisen, K.; Bjørgen, M.; Svelle, S.; Lillerud, K. P. In situ infrared spectroscopic and gravimetric characterisation of the solvent removal and dehydroxylation of the metal organic frameworks UiO-66 and UiO-67. *Top. Catal.* **2013**, *56*, 770−782.
(41) Zhu, J.; Wu, L.; Bu, Z.; Jie, S.; Li, B. G. Polyethyleneimine-modified UiO-66-NH_2 (Zr) metal-organic frameworks: preparation and enhanced CO_2 selective adsorption. *ACS Omega* **2019**, *4*, 3188−3197.
(42) Fang, Y.; Zhang, L.; Zhao, Q.; Wang, X.; Jia, X. Application of acid-promoted UiO-66-NH_2 MOFs in the treatment of wastewater containing methylene blue. *Chem. Pap.* **2019**, *73*, 1401−1411.
(43) Saleh, T. A. Simultaneous adsorptive desulfurization of diesel fuel over bimetallic nanoparticles loaded on activated carbon. *J. Clean. Prod.* **2018**, *172*, 2123−2132.
(44) Fox, B. R.; Brinich, B. L.; Male, J. L.; Hubbard, R. L.; Siddiqui, M. N.; Saleh, T. A.; Tyler, D. R. Enhanced oxidative desulfurization in a film-shear reactor. *Fuel* **2015**, *156*, 142−147.
(45) Abbaslou, R. M. M.; Tavassoli, A.; Soltan, J.; Dalai, A. K. Iron catalysts supported on carbon nanotubes for Fischer−Tropsch synthesis: Effect of catalytic site position. *Appl. Catal., A* **2009**, *367*, 47−52.
(46) Akbari, A.; Omidkhah, M.; Towfighi, D. J. Optimization of operating conditions in oxidation of dibenzothiophene in the light hydrocarbon model. *Chem. Ind. Chem. Eng. Quart.* **2014**, *20*, 315−323.
(47) Cao, Y.; Wang, H.; Ding, R.; Wang, L.; Liu, Z.; Lv, B. Highly efficient oxidative desulfurization of dibenzothiophene using Ni modified MoO_3 catalyst. *Appl. Catal., A* **2020**, *589*, 117308.
(48) Di Giuseppe, A.; Crucianelli, M.; De Angelis, F.; Crestini, C.; Saladino, R. Efficient oxidation of thiophene derivatives with homogeneous and heterogeneous MTO/H_2O_2 systems: a novel approach for, oxidative desulfurization (ODS) of diesel fuel. *Appl. Catal., B:* **2009**, *89*, 239−245.
(49) Wei, S.; He, H.; Cheng, Y.; Yang, C.; Zeng, G.; Qiu, L. Performances, kinetics and mechanisms of catalytic oxidative desulfurization from oils. *RSC Adv.* **2016**, *6*, 103253−103269.
(50) Wang, D.; Liu, N.; Zhang, J.; Zhao, X.; Zhang, W.; Zhang, M. Oxidative desulfurization using ordered mesoporous silicas as catalysts. *J. Mol. Catal. A: Chem.* **2014**, *393*, 47−55.
(51) Ren, X.; Liu, Z.; Dong, L.; Miao, G.; Liao, N.; Li, Z.; Xiao, J. Dynamic catalytic adsorptive desulfurization of real diesel over ultra-stable and low-cost silica gel-supported TiO_2. *AIChE J.* **2018**, *64*, 2146−2159.
(52) Ji, P.; Drake, T.; Murakami, A.; Oliveres, P.; Skone, J. H.; Lin, W. Tuning Lewis acidity of metal-organic frameworks via perfluorination of bridging ligands: spectroscopic, theoretical, and catalytic studies. *J. Am. Chem. Soc.* **2018**, *140*, 10553−10561.
(53) Ahmed, I.; Jhung, S. H. Effective adsorptive removal of indole from model fuel using a metal-organic framework functionalized with amino groups. *J. Hazard. Mater.* **2015**, *283*, 544−550.
(54) Chakarova, K.; Strauss, I.; Mihaylov, M.; Drenchev, N.; Hadjiivanov, K. Evolution of acid and basic sites in UiO-66 and UiO-66-NH_2 metal-organic frameworks: FTIR study by probe molecules. *Microporous Mesoporous Mater.* **2019**, *281*, 110−122.

https://doi.org/10.1021/acsomega.1c05965
ACS Omega 2022, 7, 16288−16297